Available online at www.sciencedirect.com
ScienceDirect
Optical Materials 29 (2006) 100–104
OPTICAL Materials
www.elsevier.com/locate/optmat

Indium doping in nanostructured ZnO through low-temperature hydrothermal process

A. Escobedo Morales [a], M. Herrera Zaldivar [b], U. Pal [a,*]

[a] Instituto de Física, Universidad Autónoma de Puebla, Apdo. Postal J-48, CP 72570 Puebla, Pue., Mexico
[b] Centro de Ciencias de la Materia Condensada, Universidad Nacional Autónoma de México, Apdo. Postal 2681, CP 22800 Ensenada B.C., Mexico

Available online 18 April 2006

Abstract

ZnO nanostructures of rod-like morphology were synthesized through a low-temperature hydrothermal process. Incorporation of indium in the nanostructures during synthesis was not successful due to the formation of $In(OH)_3$ phase. A post-deposition thermal annealing process in inert atmosphere resulted effective for the dissociation of $In(OH)_3$ phase and doping of indium into the nanostructures. Effect of indium doping on the structure, morphology and optical absorption of the nanostructures are studied. Beyond a certain concentration, the incorporated indium form phase separated oxide instead of being doped. Incorporated indium occupy the zinc sites in the nanostructures.

Keywords: Zinc oxide; Nanostructures; Indium doping; Hydrothermal synthesis

1. Introduction

Present interest on the development of nanostructured devices for optical, opto-electronic, electronic, and other applications have generated a huge thrust on the development of semiconductor nanostructures of adequate morphologies and compositions. While in the last decade the focus was on GaN for developing UV light emitting devices [1], recently, ZnO is considered as a potential competitor for such applications. ZnO is a semiconductor with a wide direct band gap (3.37 eV) and a large exciton binding energy (60 meV) [2] emitting blue emission in bulk form when it is pumped by an electron beam at cryogenic temperature [3,4]. In its nanostructure form, the material emits even at room temperature with low thresholds [5]. Low-dimensional nanostructures facilitate lasing by excitonic recombination since the density of states near the band gap edges is enhanced in such structures. The large exciton binding energy of ZnO further facilitate the gain mechanism [5]. An increase in the number of shallow states by adequate doping might even decrease the excitation intensity required in the ZnO nanostructures. Therefore, recently a great effort is being devoted to dope the ZnO nanostructures by several impurities like Al, Sn, Ga, In, Sb, and Cu [6–11]. Impurity doping in ZnO nanostructures mainly carried out through physical methods and the reports on the use of chemical and low-temperature synthesis routs for this purpose are rare [7,9]. The problems of opto-electronic doping through low temperature chemical synthesis techniques lie on several factors like miscibility (very different atomic/ionic radius of the guest and host), diffusion (low diffusion coefficient at low-temperature), and reactivity (formation of dopant-complexes during chemical synthesis), among others. In fact, though the ZnO nanostructures with several opto-electronic doping were prepared by physical techniques like magnetron sputtering [12,13], pulsed laser deposition [14], spray pyrolysis [5,15], vapor [16,17] and vapor–liquid–solid growth [18], or plasma induced chemical vapor deposition [19], there are not many efforts to dope ZnO nanostructures through low-temperature chemical techniques [7,9,20].

* Corresponding author. Tel.: +52 222 295500; fax: +52 222 295611.
E-mail address: upal@sirio.ifuap.buap.mx (U. Pal).

0925-3467/$ - see front matter © 2006 Elsevier B.V. All rights reserved.
doi:10.1016/j.optmat.2006.03.010

Here we report our efforts to incorporate indium in ZnO nanostructures mainly in the form of nanorods, through a low-temperature hydrothermal process. Different concentrations of indium were incorporated into the ZnO nanostructures during hydrothermal synthesis. The samples were annealed at 300 °C in argon atmosphere to observe the effect of annealing on the incorporation of indium in them. The effect of indium incorporation on the morphology, crystallinity, and composition of the samples were studied by SEM, XRD, EDS techniques. UV–Vis optical absorption spectroscopy was used to monitor the change in the optical properties of the samples.

2. Experimental

In a typical synthesis process, an alkaline solution was prepared dissolving 12 ml of ethylenediamine ($NH_2(CH_2)_2NH_2$, EDA; Baker, 99.9%) in 108 ml of ultra pure deionized water (18.0 MΩ). To the previous solution 10.25 g of zinc acetate dihydrate ($Zn(CH_3COO)_2 \cdot 2H_2O$; Aldrich, 99.99%) in powder form was added, followed by the addition of 1.70 g of sodium hydroxide (NaOH; Aldrich, 99.99%). The hydrothermal synthesis was conducted at 90 °C for 15 h in a round bottom flask using an oil bath for heating. After cooling to room temperature, the white material adhered to the reaction flask wall was extracted by decantation and dried in a muffle furnace at 80 °C for 2 h after washing by deionized water several times. For doping, a measured amount of indium chloride (III) powder ($InCl_3$; Adrich, 99.999%) was dissolved in 8 ml of deionized water from the initially measured 108 ml total. For the synthesis of the three doped samples, the aqueous solutions of $InCl_3$ with desired amounts dissolved were added to the EDA–water solution. 0.0560, 0.1067, and 0.2067 g, of $InCl_3$ were used to prepare the 0.5%, 1.0%, and 2.0% indium doped (nominal) zinc oxide samples, respectively. The later procedure was the same as for undoped sample. After the hydrothermal synthesis, the four samples were treated at 300 ° C under an argon flux for 2 h. The ZnO nanostructures were characterized by X-ray diffraction (XRD) (Phillips X'Pert diffractometer with Cu Kα radiation), scanning electron microscopy (SEM) (Jeol JSM 5300), energy dispersive X-ray spectroscopy (EDS) (Thermo Noran Super dry II) and UV–Vis absorption spectroscopy (Shimadzu, UV-3101PC double beam spectrophotometer) techniques. For absorption measurements, the powder samples were dispersed in deionized water with same concentration for all the samples and the spectra were recorded at room temperature.

3. Results and discussion

From the SEM micrographs (Fig. 1), we can see the formation of rod-like morphology of the undoped and doped nanostructures. Most of the nanostructures remained grouped to form a flower-like morphology. The needle shaped nanorods were of 450 nm average diameter and of 5.0 μm average length. There was no remarkable difference between the morphologies of the as-grown doped and undoped samples.

The XRD spectra of the as-grown samples (doped and undoped) are presented in Fig. 2. We can observe the appearance of prominent diffraction peaks related to wurtzite ZnO in all the samples. The intensity of the XRD peaks increased to some extent on incorporation of 0.5% In, but decreased gradually on increasing the In concentration. The initial increase of ZnO peak intensity might be due to the incorporation of In in the interstitial sites of ZnO lattice. However a higher doping concentration causes the nanostructures poorly crystalline.

There appeared some extra peaks related to $In(OH)_3$. The presence of $In(OH)_3$ related peaks in the XRD spectra indicate that the added indium instead of being doped into ZnO, remained phase separated, at least partially.

To reduce the $In(OH)_3$ phase in the samples, we annealed all the samples at 300 °C in argon for 2 h. As expected, the XRD spectra of the annealed samples did not reveal any diffraction peak related to $In(OH)_3$. However, the morphology of the indium incorporated samples drastically changed (Fig. 3). The presence of indium in the doped samples after annealing was monitored through EDS analysis (Fig. 4). The results of EDS elemental analysis are presented in Table 1. For all the dopes samples, the estimated indium concentrations were a bit higher than their corresponding nominal values. Apart from that, the increase of indium concentration in the samples caused a

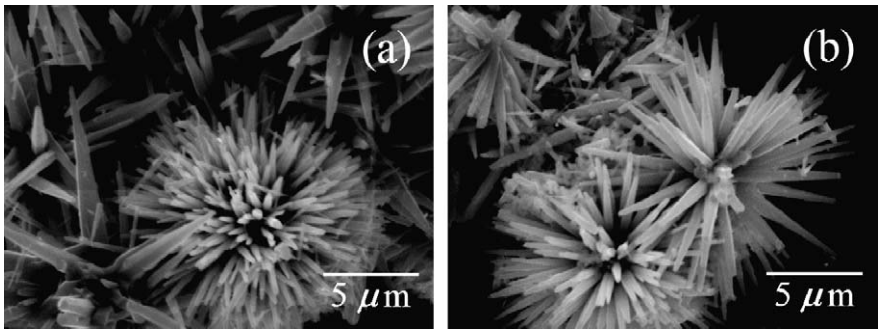

Fig. 1. Typical SEM micrographs of the as-grown (a) undoped and (b) 2.0% indium doped ZnO nanostructures.

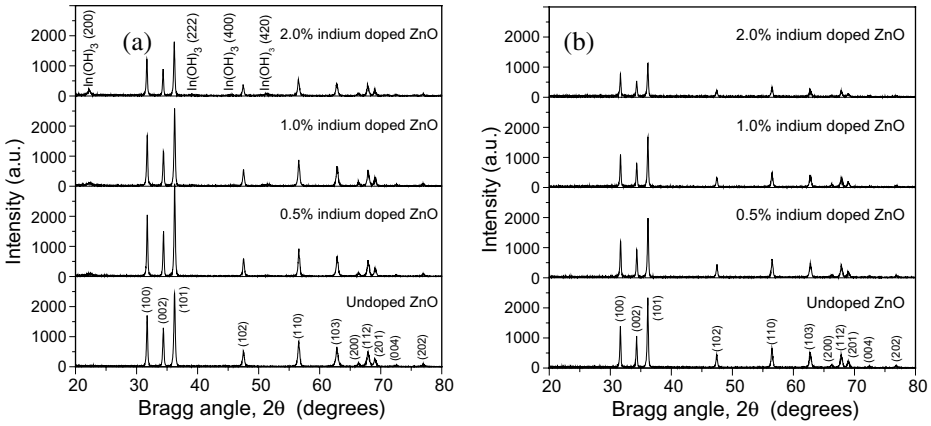

Fig. 2. XRD patterns of the ZnO nanostructures (a) before and (b) after thermal annealing.

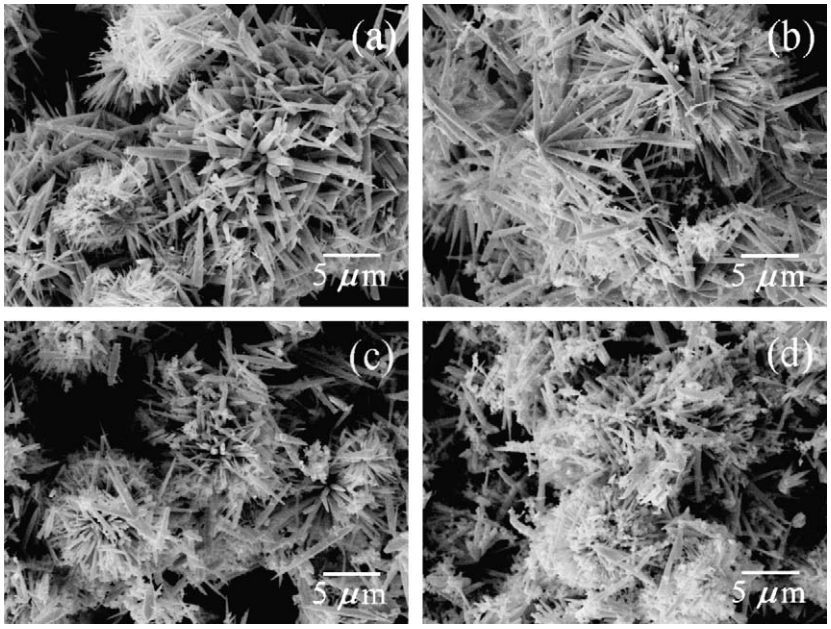

Fig. 3. Typical SEM micrographs of the annealed samples; (a) undoped ZnO, (b) 0.5% indium doped ZnO, (c) 1.0% indium doped ZnO, and (d) 2.0% indium doped ZnO.

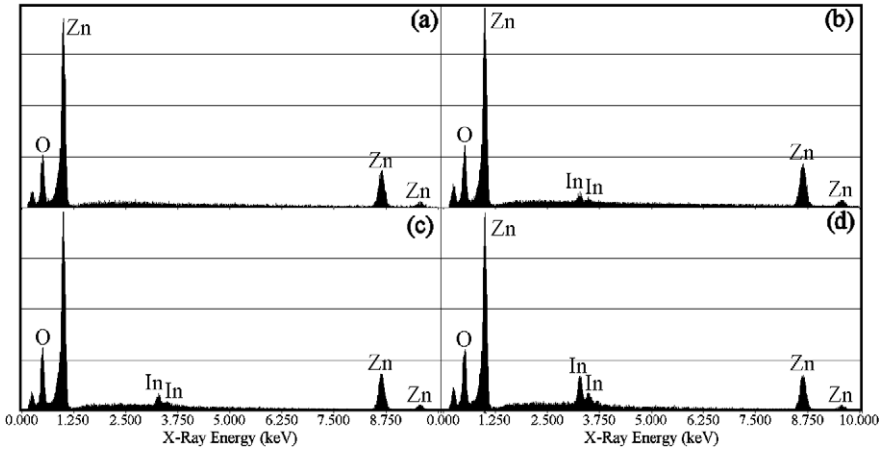

Fig. 4. EDS spectra of the annealed; (a) undoped, (b) 0.5% indium doped, (c) 1.0% indium doped, and (d) 2.0% indium doped ZnO nanostructures.

Table 1
EDS composition and positions of the main diffraction peaks for the annealed samples

Nominal In concentration in the sample (%)	Zn:O:In, at.% (EDS average)	(002) diffraction peak position and FWHM (degrees)	(100) diffraction peak position (degrees)
0.0	50:50:0	34.33 (0.19)	31.66
0.5	49.15:50.17:0.68	34.34 (0.20)	31.69
1.0	48.45:50.31:1.24	34.33 (0.20)	31.67
2.0	46.11:50.78:3.11	34.32 (0.22)	31.66

The FWHM of the (002) diffraction peak is given in parenthesis.

systematic decrease of zinc concentration indicating the replacement of Zn atoms in the lattice sites by In atoms. Therefore, it is reasonable to consider that the indium in the samples incorporated as in the annealed nanostructures through substitutional doping.

The effect of indium incorporation in the ZnO lattice was studied by monitoring the position and broadening of the diffraction peaks in the XRD spectra. Though the intensity of the diffraction peaks was affected severely on incorporation of indium, except a small shift in position towards lower angles, there were not much change in the peak positions or their widths. Such a small shift of peak position might be due to the deformation of ZnO lattice due to incorporation of In ions of bigger ionic radius [$r(Zn^{2+}) = 74$ pm and $r(In^{3+}) = 76$ pm] [6,21]. In Table 1 the position of the prominent XRD peaks and their FWHM are presented.

While there was not much deformation of lattice due to indium incorporation in the nanostructures, their morphology modified drastically. Fig. 3 demonstrates clearly that the nanostructures are no more flower-like after annealing. Formation of particle-like (140 nm average diameter) structures dispersed in the sample is clear in the SEM images. Moreover, a close observation can reveal that the surface of the rod-like nanostructures are no more smooth after annealing the doped samples. The results clearly indicate the effect of indium incorporation on the morphology and crystallinity of the ZnO nanostructures. Formation of particle-like structures and granular surface of nanorods justify well for the reduction of XRD peak intensities in the doped samples after annealing. The EDS spectra of the doped and undoped nanostructures are shown in Fig. 4.

To study the homogeneity of indium distribution in the doped samples after annealing, we acquired backscattered electron images of the samples in SEM (Fig. 5). Backscattered electron images of the samples revealed almost an uniform distribution of incorporated indium in the nanostructures. However, there were some local agglomerates formed by the particle-like structures for heavily doped (2%) samples (shown by a circle in the Fig. 5c). On analyzing those local areas by EDS and comparing them with the general EDS spectra of the sample (Fig. 5b and d) we could see that the agglomerated areas are of high indium content and also richer in oxygen (Zn:O:In (at.%) = 21.61: 58.25:20.14). We believe that such agglomerated structures are indium oxide formed with the indium in excess of dop-

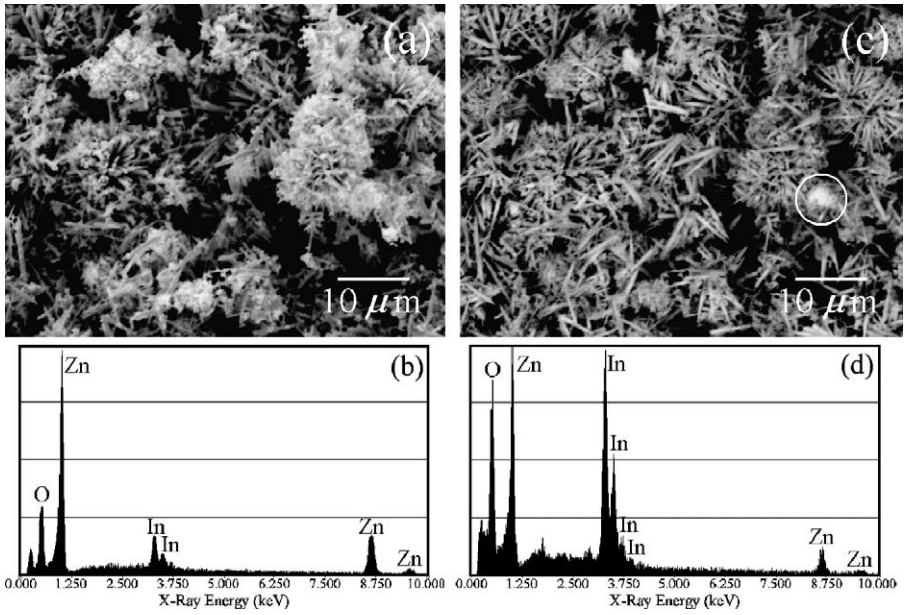

Fig. 5. SEM images of 2.0% indium (nominal) incorporated sample in (a) secondary and (b) backscattered modes. The EDS spectra of the sample over a wide area and at a selected area (circle marked in c) are shown in (b) and (d), respectively.

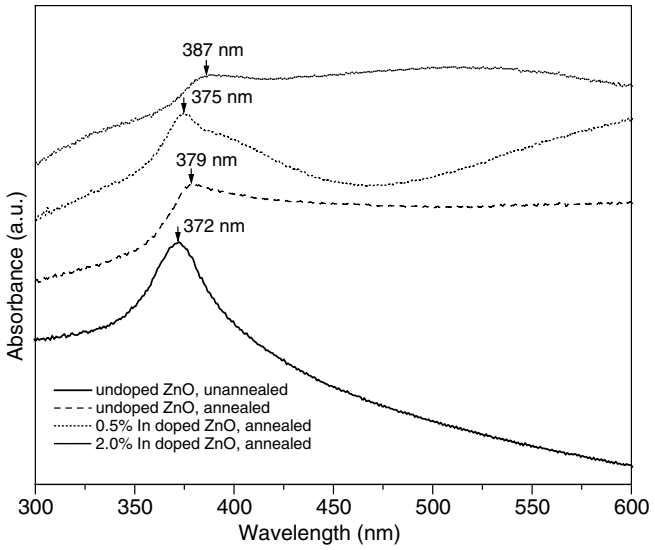

Fig. 6. UV–Vis absorption spectra of doped and undoped samples after thermal annealing. For comparison, the absorption spectrum of the as-grown undoped sample is included.

ing. However, to know the exact composition of such oxide a further analysis is needed.

The optical properties of the ZnO nanostructures were studied by UV–Vis absorption spectroscopy. Absorption spectra of the doped and undoped annealed nanostructures are presented in Fig. 6. For reference, the absorption spectrum of the as-grown undoped sample is also presented. We can see the appearance of an absorption peak at about 372 nm (3.33 eV) in the as-grown undoped ZnO nanostructures. After annealing, the peak shifted slightly towards higher wavelength (379 nm, 3.27 eV), which might be due to relaxation of growth induced strain in them. On incorporation of 0.5% indium, the absorption peak shifted a bit towards lower wavelength (375 nm, 3.31 eV), but shifted towards higher wavelength for higher In contents. Though there was not much variation in the peak position of the absorption band on indium doping, from the figure, we can see that the background absorption at the higher wavelengths increased drastically. Such an increase in background absorption is due to higher scattering of light at the rough surfaces of the doped nanostructures.

4. Conclusions

On summarizing the presented results, we can conclude that the doping of In in ZnO nanostructures through low-temperature hydrothermal process is difficult. The most of the In ions in the mixture solution forms $In(OH)_3$ and remain as a separate phase in the samples. The dissociation of $In(OH)_3$ phase and thereby partial incorporation of In in ZnO nanostructures is possible through annealing the samples at 300 °C in inert atmosphere. For a lower concentration, the incorporated In distribute uniformly in the nanostructures, but for higher concentrations, the excess In forms its oxide and remains phase separated. The morphology of ZnO nanostructures change drastically on the incorporation of indium. The nanostructures loose their crystallinity, forming granular surface and particle-like morphologies. Incorporated indium in ZnO nanostructures substitutes zinc from its lattice sites. The mechanism of formation of nanoparticles on indium doping and thermal annealing needs further studies.

Acknowledgements

We are thankful to E. Aparicio Ceja and I. Gradilla Martinez, CCMC-UNAM for their helps in XRD and SEM measurements of the nanostructures. The work is partially supported by CONACyT, Mexico (Grant No. 4626) and UC-MEXUS-CONACyT (Grant No. CN-05-215).

References

[1] S. Nakamura, M. Senoh, S. Nagahama, N. Iwasa, T. Yamada, T. Matsushita, Y. Sugimoto, H. Kiyoku, Appl. Phys. Lett. 69 (1996) 1477.
[2] C. Klingshirn, Phys. Status Solidi B 71 (1975) 547.
[3] F.H. Nicoll, Appl. Phys. Lett. 9 (1996) 13.
[4] J.M. Hvam, Solid State Commun. 12 (1973) 95.
[5] J.C. Johnson, H. Yan, R.D. Schaller, L.H. Haber, R.J. Saykally, P. Yang, J. Phys. Chem. B 105 (2001) 11387.
[6] S.Y. Bae, C.W. Na, J.H. Kang, J. Part, J. Phys. Chem. B 109 (2005) 2526.
[7] S.B. Majumder, M. Jain, P.S. Dobal, R.S. Katiyar, Mater. Sci. Eng. B 103 (2003) 16.
[8] C. Xu, M. Kim, J. Chun, D. Kim, Appl. Phys. Lett. 86 (2005) 133107.
[9] Th. Agne, Z. Guan, X.M. Li, H. Wolf, Th. Wichert, H. Natter, R. Hempelmann, Appl. Phys. Lett. 83 (2003) 1204.
[10] J. Zuo, C. Xu, L. Zhang, B. Xu, R. Wu, J. Raman Spectrosc. 32 (2001) 979.
[11] C.X. Xu, X.W. Sun, X.H. Zhang, L. Ke, S.J. Chua, Nanotechnology 15 (2004) 856.
[12] K. Zhang, F. Zhu, C.H.A. Huan, A.T.S. Wee, T. Osipowicz, Surf. Interface Anal. 28 (1999) 271.
[13] R. Wang, L.H. King, A.W. Sleight, J. Mater. Res. 11 (1996) 1659.
[14] M. Yan, H.T. Zhang, E.J. Widjaja, R.P.H. Chang, J. Appl. Phys. 94 (2003) 5240.
[15] A. Maldonado, M.L. Olvera, R. Asomoza, E.P. Zironi, J. Cañetas-Ortega, J. Palacios-Gomez, J. Vac. Sci. Technol. 15 (1997) 2905.
[16] C.X. Xu, X.W. Sun, B.J.P. Chen, Appl. Phys. Lett. 84 (2004) 1540.
[17] J.Y. Lao, J.G. Wen, Z.F. Ren, Nano Lett. 2 (2002) 1287.
[18] S.Y. Li, P. Lin, C.Y. Lee, T.Y. Tseng, C.J. Huang, J. Phys. D-Appl. Phys. 37 (2004) 2274.
[19] S.Y. Bae, H.W. Seo, J. Park, J. Phys. Chem. B 108 (2004) 5206.
[20] S. Huang, T. Kaydanova, A. Miedaner, D.S. Ginley, J. Undergraduate Res. 4 (2004) 70 (US Department of Energy, Office of Science).
[21] R.D. Shannon, Acta Cryst. A 32 (1976) 751.